

biniLasso: Automated cut-point detection via sparse cumulative binarization

Abdollah Safari*

School of Mathematics, Statistics, and Computer Science, College of Applied Sciences, University of Tehran, Iran,
*email: a.safari@ut.ac.ir

and

Hamed Helisaz

Department of Statistics, Faculty of Science, University of British Columbia, Vancouver, Canada
GranTAZ Consulting LTD, Vancouver, Canada

and

Peter Loewen

Faculty of Pharmaceutical Sciences, University of British Columbia, Canada

SUMMARY: We present biniLasso and its sparse variant (sparse biniLasso), novel methods for prognostic analysis of high-dimensional survival data that enable detection of multiple cut-points per feature. Our approach leverages the Cox proportional hazards model with two key innovations: (1) a cumulative binarization scheme with L_1 -penalized coefficients operating on context-dependent cut-point candidates, and (2) for sparse biniLasso, additional uniLasso regularization to enforce sparsity while preserving univariate coefficient patterns. These innovations yield substantially improved interpretability, computational efficiency ($4\text{--}11\times$ faster than existing approaches), and prediction performance. Through extensive simulations, we demonstrate superior performance in cut-point detection, particularly in high-dimensional settings. Application to three genomic cancer datasets from TCGA confirms the methods' practical utility, with both variants showing enhanced risk prediction accuracy compared to conventional techniques. The biniLasso framework thus provides a powerful, flexible tool for survival analysis in biomedical research.

KEY WORDS: Feature binarization; optimal cut-points; L_1 norm penalty; Lasso; sparse regression; survival analysis; high-dimensional.

1. Introduction

The discretization of continuous predictors is a cornerstone of interpretable modeling in clinical and epidemiological research, where simplicity and actionability often outweigh granular precision. Diverse applications from heart rate thresholds in pulmonary disease (Philip et al., 2000) to medication adherence in atrial fibrillation patients (Safari et al., 2024; Salmasi et al., 2024) require statistically sound approaches to identify optimal cut-points for discretization. While thresholds such as 'heart rate $> 100bpm$ ' or 'medication adherence $> 80\%$ ' are entrenched in clinical practice, they are often derived from expert consensus or arbitrary quantiles, risking suboptimal power or missed biological signals. Modern high-dimensional datasets demand data-driven cut-point detection methods that balance interpretability with predictive accuracy, particularly within sparse regression frameworks like the Lasso.

Current approaches to cut-point detection mostly suffer from key limitations. Methods based on multiple testing (e.g., Bland and Altman 1995; Lausen and Schumacher 1992) are computationally inefficient, often restricting analysis to a small set of candidate thresholds and potentially missing optimal cut-points. Other approaches focus solely on single-

predictor settings (e.g., O'Brien 2004), rendering them inadequate for high-dimensional data where joint selection and thresholding of multiple variables is essential.

To our knowledge, the only existing scalable statistical approach for data-driven cut-point detection is the Binacox method by Bussy et al. (2022). This method addresses automatic cut-point identification in high-dimensional Cox models, particularly relevant for medical and genetic studies where multiple cut-points per feature are often needed (e.g., Cheang et al. 2009). Binacox employs one-hot encoding (Wu and Coggeshal, 2012) combined with the binarsity penalty Alaya et al. 2019 - a total-variation regularization with an additional linear constraint - to simultaneously perform feature selection while maintaining interpretability. This framework enables automatic detection of cut-points in continuous features, facilitating both the understanding of nonlinear effects and the development of predictive risk scores. The authors demonstrated the theoretical robustness of the Binacox method by establishing nonasymptotic oracle inequalities for prediction and estimation. They also validated the method through extensive simulations and applications to high-dimensional genetic cancer datasets. The results showed that Binacox outperforms two classical approaches, both based on multi-

ple log-rank tests but with different corrections for multiple testing (Bland and Altman 1995; Lausen and Schumacher 1992), in terms of risk prediction and computational efficiency, making it a compelling tool for clinical research and practical implementation in prognostic studies.

Despite its strengths, the Binacox method has some limitations that warrant consideration. The Binacox theoretical results rely on the assumption that true cut-points exist (Assumption 3 in Bussy et al. 2022), implying that the true relationship between a continuous predictor and the outcome can be fully represented through the predictor’s categorical version with unknown cut-points. While this assumption is necessary for deriving theoretical results, its practical implications remain unexplored. Binacox’s performance in real-world settings, where such an assumption may not hold, has not been investigated, as Bussy et al. (2022) only evaluated the method in simplified scenarios with true cut-points. A key consequence of this assumption is Binacox’s reliance on abrupt effect changes for cut-point detection. When violated (e.g., when a covariate’s effect shifts gradually), the method may miss meaningful thresholds or overfit, generating excessive spurious cut-points in smoothly varying regions. Another constraint of the Binacox method emerges from its binarization approach, which requires adequate sample sizes within each generated bin for reliable effect estimation. The conventional dichotomization process creates indicator variables at identified cut-points, but this formulation becomes unstable when analyzing regions where either the covariate’s effect changes occur in sparsely sampled ranges, or multiple cut-points are detected in close proximity, producing undersized bins. This sample density dependence particularly hinders the method’s ability to detect important cut-points in unevenly distributed covariates. Finally, Binacox model’s disregard for the impact of covariate boundary values may lead to an overemphasis on local effects, neglecting the overall trend of a covariate’s influence. This limitation becomes particularly problematic in the presence of inflated observations near the boundaries, which can result in the identification of suboptimal cut-points that fail to accurately capture the broader effect of the covariate across its entire range. For example, the proportion of days covered (PDC) is commonly used to estimate medication adherence by calculating the proportion of days during a specific period in which a person has access to the medication. PDC, as a continuous metric within $[0, 1]$, is often treated as the primary exposure in studies aiming to assess its effect on outcomes. Notable examples include Safari et al. (2024) and Salmasi et al. (2024), where PDC for oral anticoagulants was used to evaluate major clinical outcomes in patients with atrial fibrillation. The distribution of PDC in this population typically exhibits two peaks, at $\text{PDC}=0$ and $\text{PDC}=1$, a pattern often observed in other populations due to the nature of PDC. Applying Binacox model in such cases may lead to the identification of cut-points near these inflated boundary values, such as $\text{PDC}=0$ and $\text{PDC}=1$, driven by the distribution rather than the covariate’s true effect. Consequently, this undermines the model’s ability to capture meaningful changes in PDC effects across its full range.

In this work, we introduce *biniLasso*, a new approach to cut-point detection that addresses key limitations of existing methods like Binacox. While Binacox relies on one-hot encod-

ing, *biniLasso* employs cumulative binarization, a paradigm shift that more accurately captures the underlying effects of continuous covariates. This framework not only improves cut-point detection but also naturally aligns with clinical interpretation, where risk thresholds (e.g., ‘above/below a critical value’) are more meaningful than discrete categories. Additionally, we proposed sparse *biniLasso* by integrating the recently developed *uniLasso* method, which enforces sparsity while preserving the sign of univariate model coefficients and their magnitude (Chatterjee et al., 2025). This dual innovation, cumulative binarization plus *uniLasso*, ensures both interpretability (via threshold-aligned effects) and statistical efficiency (via sparse, univariate-consistent estimates).

Given the importance of Cox models in clinical research and to enable direct comparison with Bussy et al. (2022)’s findings, we focus our implementation on survival analysis and specifically on Cox models. However, our approach can be readily extended to generalized linear models (GLMs). We validate the effectiveness of this approach through an extensive simulation study encompassing a wide range of scenarios, from the presence of true cut-points to more complex and gradual effects of continuous predictors on outcomes. These results underscore the potential of *biniLasso* to improve the interpretability and utility of survival models, especially in high-dimensional settings. Finally, we illustrate the method’s practical utility by applying it to three high-dimensional cancer genomics datasets previously analyzed by Bussy et al. (2022).

The remainder of this paper is structured as follows: Section 3 provides a review of the Binacox method along with a detailed presentation of our proposed *biniLasso* approach. Section 4 discusses implementation of our method in an R statistical package. In Section 5, we report the results of a comprehensive simulation study to evaluate the performance of our method. In Section 6, we demonstrate *biniLasso*’s practical utility through a case study using three high-dimensional cancer genomics datasets, the same datasets analyzed in the Binacox paper. These datasets were also used in Binacox paper. Finally, Section 7 presents the discussion and conclusions, summarizing key findings and potential future research directions.

2. Notation

We present the *biniLasso* approach, including its binarization modification step, estimation procedure, and implementation details. To maintain consistency, we adopt the notation used by Bussy et al. (2022) to describe the variables and models. Specifically, let $(X_i, Z_i, \Delta_i) \in \prod_{j=1}^p [a_j, b_j]^p \times \mathbb{R}^+ \times \{0, 1\}$, for $i = 1, \dots, n$, where the boundary values a_j and b_j of the j^{th} predictor may extend to $-\infty$ and ∞ , respectively. If population-level minimum and maximum values of the predictors were available, one could normalize the predictors accordingly, simplifying the notation by setting $a_j \equiv 0$ and $b_j \equiv 1$.

The Cox proportional hazards model (Cox, 1972) is used to describe the relationship between the hazard function and predictor variables, modelled as:

$$\lambda(t|X_i) = \lambda_0(t) \exp(f(X_i)) \quad (1)$$

where $\lambda_0(t)$ is the baseline hazard function, and $f(\cdot)$ quantifies the relationship between the covariates X_i and the outcome hazard. The primary objective is to estimate the function $f(\cdot)$.

3. Method

3.1 Review of Binacox

Before introducing the proposed biniLasso approach, we briefly review the Binacox method by Bussy et al. (2022). In the Binacox method, the covariates are transformed into a sparse binarized matrix X^B , where continuous variables are one-hot encoded (Wu and Coggeshal, 2012). This encoding expands the original matrix into $p+d$ columns, possibly $d \gg p$, where the j^{th} continuous feature is replaced by $d_j + 1 \geq 2$ binary columns $X_{\cdot,j,1}^B, \dots, X_{\cdot,j,d_j+1}^B$, and $d = \sum_{j=1}^p d_j$.

The intervals $I_{j,1}, \dots, I_{j,d_j+1}$ partition the range of the j^{th} continuous covariate such that for each observation $i = 1, \dots, n$ and for each feature j , the binarized covariate $X_{i,j,l}^B$ is defined as:

$$X_{i,j,l}^B = \begin{cases} 1 & \text{if } X_{i,j} \in I_{j,l} \\ 0 & \text{otherwise,} \end{cases}$$

The function $f(\cdot)$ is then represented as:

$$f_\beta(X_i) = \beta^T \mathbf{X}_i^B = \sum_{j=1}^p f_{\beta_{j,\cdot}}(X_{i,j}) = \sum_{j=1}^p \sum_{l=1}^{d_j+1} \beta_{j,l} \mathbf{1}(X_{i,j} \in I_{j,l}) \quad (2)$$

where the vector of coefficients β is given by:

$$\begin{aligned} \beta &= (\beta_1^T, \dots, \beta_p^T)^T \\ &= (\beta_{1,1}, \dots, \beta_{1,d_1+1}, \dots, \beta_{p,1}, \dots, \beta_{p,d_p+1})^T \end{aligned} \quad (3)$$

To estimate the parameters β , the method employs a penalized partial likelihood approach with a constrained total variance penalty term (a group fused lasso like penalty). Specifically, the optimization problem can be expressed as follows:

$$\hat{\beta} = \underset{\beta \in \mathfrak{B}_{p+d}(C)}{\operatorname{argmin}} \{l_n(f_\beta) + \operatorname{bina}(\beta)\} \quad (4)$$

where $\mathfrak{B}_{p+d}(C) = \{\beta \in R^{p+d} : \sum_{j=1}^p \|\beta_{j,\cdot}\|_\infty \leq C \text{ \& } n_{j,\cdot}^T \beta_{j,\cdot} = 0\}$ and $n_{j,\cdot}$ is the vector of number of observations corresponding to the intervals of the j^{th} predictor ($I_{j,1}, \dots, I_{j,d_j+1}$). Then, the scaled negative log-partial likelihood function is:

$$l_n(f_\beta) = -\frac{1}{n} \sum_{i=1}^n \Delta_i \left\{ f_\beta(X_i) - \log \sum_{i': Z_{i'} \geq Z_i} \exp(f_\beta(X_{i'})) \right\} \quad (5)$$

and the binarization penalty is:

$$\operatorname{bina}(\beta) = \sum_{j=1}^p \left(\sum_{l=2}^{d_j+1} w_{j,l} |\beta_{j,l} - \beta_{j,l-1}| \right) \quad (6)$$

where $w_{j,l}$'s are a set of data-driven weights to scale contributing covariates' effects in the penalty term (see Gaïffas and Guillaux 2012 for more details). This formulation encourages smooth transitions between adjacent cut-points while penalizing large differences in the coefficients, aiming an interpretable and sparse solution.

3.2 Cumulative binarization

To achieve a more accurate proxy for capturing the effect of continuous covariates through their categorized counterparts, we adopt a modified binarization technique. Unlike conventional binarizations that rely on standard one-hot encoding, we propose a novel approach termed cumulative binarization. This method begins by partitioning the domain of continuous covariates into multiple disjoint bins. However, instead of generating a separate indicator variable for each bin, we construct dummy variables that cumulatively represent the region beyond each splitting point. Specifically, each dummy variable corresponds to an interval defined by a splitting value, with larger splitting values nested within intervals created by smaller splitting points.

Let X^B represent the (possibly sparse) binarized matrix with $p+d$ columns, where continuous features are cumulatively one-hot encoded. Unlike Binacox, we relax the assumption of known population-level minimum and maximum values for the predictors X to rescale them to $[0, 1]$. Continuous predictors can still be standardized (or normalized) based on the sample data before fitting the model, as is common when penalty terms involve the absolute values of predictor coefficients. Importantly, these preprocessing steps do not require access to population-level data.

For the j^{th} feature with $d_j + 1$ cumulative binarized columns, we define strictly increasing endpoints $\mu_{j,l}, l = 0, \dots, d_j$ (potential cut-points). These endpoints create nested, decreasing intervals $I_{j,l}^c = (\mu_{j,l}, b_j]$ for $l = 0, \dots, d_j$, with $I_{j,0}^c = (a_j, b_j]$. For each observation $i = 1, \dots, n$ and $l = 0, \dots, d_j$, the cumulative binarized variable $X_{i,j,l}^{CB}$ is then defined as:

$$X_{i,j,l}^{CB} = \begin{cases} 1 & \text{if } X_{i,j} \in I_{j,l}^c, \\ 0 & \text{otherwise} \end{cases} \quad (7)$$

Additionally, let $\mathbf{X}_{j,l}^{CB}$ be the vector of the l^{th} cumulative binarized column corresponds to the j^{th} feature.

The rationale behind this cumulative binarization is to facilitate the interpretation of the j^{th} continuous covariate at each cut-point by comparing “lower versus all higher values”: values in $(a_j, \mu_{j,l}]$ (“lower”) vs values in the complement of that interval (“all higher”). This enables the direct estimation of the effect size for such low/high comparisons. By simultaneously including multiple cumulative binarized covariates, we can comprehensively perform comparisons across different intervals of the continuous covariate, providing a richer understanding of the variable's relationship to the outcome.

3.3 Estimation procedure

For each binarized feature $\mathbf{X}_{j,l}^{CB}$, there corresponds a parameter $\beta_{j,l}^*$. The vector associated with the binarization of the j^{th} feature is denoted by $\beta_j^* = (\beta_{j,1}^*, \dots, \beta_{j,d_j}^*)^T$. Each parameter $\beta_{j,l}^*$ is linked to a corresponding cut-point $\mu_{j,l}$, thus the parameter vector β_j^* corresponds to the cut-point vector $\boldsymbol{\mu}_j = (\mu_{j,1}, \dots, \mu_{j,d_j})^T$. Using this parameterization, a candidate function for the estimation of f , denoted as f^* , can

be expressed as:

$$\begin{aligned} f_{\beta^*}(\mathbf{X}_i) &= \beta^{*T} \mathbf{X}_i^{CB} = \sum_{j=1}^p f_{\beta_j^*}(X_{i,j}) \\ &= \sum_{j=1}^p \sum_{l=1}^{d_j} \beta_{j,l}^* \mathbf{1}(X_{i,j} \in CI_{j,l}) \end{aligned} \quad (8)$$

where the full parameter vectors of size $p + d$ and d , respectively, are obtained by concatenating the vectors β_j^* and μ_j , similar to the formulation in Eq. (3).

To estimate the parameter β^* , we apply a weighted lasso penalized partial likelihood approach. The optimization problem is defined as:

$$\hat{\beta}^* = \underset{\beta^*}{\operatorname{argmin}} \left\{ \ln(f_{\beta^*}) + \sum_{j=1}^p \left(\sum_{l=1}^{d_j+1} w_{j,l}^* |\beta_{j,l}^*| \right) \right\} \quad (9)$$

While assigning different weights $w_{j,l}^*$ to each parameter $\beta_{j,l}^*$ as additional tuning constants enhances model flexibility, it comes at the cost of increased computational complexity during model fitting. As an alternative, these weights can be specified using strategies similar to those employed in group and adaptive Lasso techniques (e.g., cross validation). Since interpretability is our primary goal, many applications prefer a limited number of levels when categorizing continuous covariates. For such cases, these weights can be strategically specified based on the data to achieve a predefined number of levels for each covariate. Therefore, one can simplify the penalty term as:

$$\sum_{j=1}^p w_j^* \left(\sum_{l=1}^{d_j+1} |\beta_{j,l}^*| \right), \quad (10)$$

where w_j^* is a weight (not necessarily unique) that returns exactly a fixed predefined number of $\beta_{j,l}^*$'s non-zero for the j^{th} feature. This simplification balances model flexibility with practical considerations, maintaining interpretability while reducing complexity.

3.4 *biniLasso* vs *Binacox*

Comparing our proposed cumulative intervals $CI_{j,l}$ with those in *Binacox*, we observe that $CI_{j,l} = \bigcup_{i=l}^{d_j+1} I_{j,i}$, which implies that $\mathbf{1}(X_{i,j} \in CI_{j,l}) = \sum_{k=l}^{d_j+1} \mathbf{1}(X_{i,j} \in I_{j,k})$. Furthermore, the partial likelihood function $\ln(f_{\beta^*})$ depends on the parameter vector β^* only through the function f , with f_{β^*} serving as a reparameterization of f_{β} . Specifically, for $j = 1, \dots, p$ and $i = 1, \dots, n$, the function $f_{\beta_j^*}(X_{i,j})$ can be expressed as:

$$f_{\beta_j^*}(X_{i,j}) = \sum_{l=1}^{d_j+1} \beta_{j,l}^* \mathbf{1}(X_{i,j} \in CI_{j,l}) \quad (11)$$

$$= \sum_{l=1}^{d_j+1} \beta_{j,l}^* \sum_{k=l}^{d_j+1} \mathbf{1}(X_{i,j} \in I_{j,k}) \quad (12)$$

$$= \sum_{k=1}^{d_j+1} \mathbf{1}(X_{i,j} \in I_{j,k}) \sum_{l=k}^{d_j+1} \beta_{j,l}^*. \quad (13)$$

By comparing this expression with the formulation of f in the *Binacox* model (Eq. 2), it can be established that setting $\beta_{j,k} = \sum_{l=k}^{d_j+1} \beta_{j,l}^*$ confirms $f_{\beta_j^*}(X_{i,j})$, and consequently $f_{\beta_j^*}$, as a reparameterization of $f_{\beta_j}(X_{i,j})$ and f_{β_j} . Furthermore, the relationship between the β^* parameters and the β parameters implies that the binarization penalty term (originally a group fused lasso-like penalty) simplifies to the more standard group lasso penalty term, offering computational and conceptual advantages.

Our *biniLasso* model parametrization offers several advantages. First, the objective function of *biniLasso* resembles that of a Cox model with an ℓ_1 norm penalty (lasso, achieved by setting all weights to one). This structure allows *biniLasso* to be easily and efficiently fitted using commonly available statistical packages, unlike *Binacox*. Second, while Bussy et al. (2022) introduced explicit, data-driven expressions for the weights $w_{j,l}$ (dependent on a single tuning parameter) that are optimal only under specific, and sometimes unrealistic, assumptions (e.g., Assumption 3 in Bussy et al. 2022). On the other hand, treating these weights as additional tuning parameters in *Binacox* is computationally challenging due to its non-conventional penalty term. In contrast, *biniLasso* employs a more conventional penalty structure, enabling all weights to be treated as tuning parameters while still allowing efficient estimation using readily available libraries in R or Python. Finally, and perhaps most importantly, the definition of the coefficients β^* , which directly focus on low/high comparisons, enhances the interpretability of the estimated covariate effects, providing a clearer and more intuitive understanding of their impact.

3.5 *Feature boundaries*

An important application of categorizing a continuous covariate is the identification of thresholds, such as risk thresholds, where values below or above a specific cut-point are interpreted similarly to boundary values in terms of their impact on the outcome. This type of interpretation is particularly relevant for predictors with known population-level minimum and maximum values. For instance, given a threshold μ_j^* for a scaled covariate $X_{.,j} \in [0, 1]$ by setting $a_j \equiv 0$ and $b_j \equiv 1$, the interpretation might be that, while holding all other covariates constant, any observation with $X_{.,j} \in (0, \mu_j^*)$ is considered to have a comparable outcome risk to those with $X_{.,j} = 0$.

In this context, the problem of finding the optimal threshold for dichotomizing $X_{.,j}$ becomes equivalent to identifying the maximum (or minimum) value of $X_{.,j}$, denoted μ_j^* , such that observations with $X_{.,j} \in (0, \mu_j^*)$ (or $X_{.,j} \in (\mu_j^*, 1]$) would have a similar outcome as those with $X_{.,j} = 0$ (or $X_{.,j} = 1$), while other predictors in the model remain fixed.

The focus here is not on assessing the impact of the covariate at its boundary values, but rather on identifying which middle values in $(0, 1)$ exhibit a similar effect to that at the boundaries. To account for the boundaries explicitly, two indicator variables can be introduced for the boundary values of the covariate:

$$X_{i,j,bl} = \begin{cases} 1 & \text{if } X_{i,j} = l, \\ 0 & \text{otherwise,} \end{cases} \quad (14)$$

where $l \in \{0, 1\}$. These boundary indicators are included in the model but are excluded from the penalty term during regularization. The role of regularization, in this case, is to control the number of intervals within $(0, 1)$ that show distinct effects on the outcome, while adjusting for the boundary values. This technique proves especially useful in cases where observations are disproportionately concentrated near the covariate boundaries, helping the model to distinguish between the effect of boundary values and the effect of values near the boundary.

3.6 Sparse biniLasso

While the Lasso has been widely adopted in many applications, it suffers from well-known limitations, particularly its sensitivity to correlated predictors. This issue is especially relevant in our context, as cumulative binarization inherently creates correlated features. To address this challenge while maintaining both sparsity and interpretability, we incorporate uniLasso (Chatterjee et al., 2025), a novel two-stage regularized regression approach. The uniLasso procedure consists of three key steps:

- First, fit univariate Cox models for each individual indicator variable of each binarized feature, generating linear predictor functions $\hat{\eta}_{j,l}(x_{i,j,l})$ for $j = 1, \dots, p$ and $l = 1, \dots, d_j$
- Next, compute leave-one-out (LOO) predictions $\hat{\eta}_{j,l}^{-i}$ for all n observations and each (j, l) pair
- Finally, fit a non-negative Lasso Cox model using these LOO predictions as features

This two-stage approach provides important theoretical and practical advantages. First, the univariate Cox models (Step 1) and non-negative Lasso Cox model (Step 3) together ensure sign consistency, i.e., the estimated coefficients in the multivariable model preserve the direction of effects from their univariate counterparts. Second, by design, this approach maintains comparable coefficient magnitudes between univariate and multivariable models without requiring feature standardization in Step 3. Finally, using leave-one-out predictions (Step 2) enhances the robustness and predictive performance of the final multivariate model by reducing overfitting (Chatterjee et al., 2025). This leads to the modified optimization problem:

$$\hat{\theta} = \underset{\theta}{\operatorname{argmin}} \left\{ l_n(f_{\theta}) + \sum_{j=1}^p \left(\sum_{l=1}^{d_j+1} w_{j,l}^{**} |\theta_{j,l}| \right) \right\} \quad (15)$$

subject to $\theta_{j,l} \geq 0$ for all j and l , where $f_{\theta}(\mathbf{X}_i) = \sum_{j=1}^p \sum_{l=1}^{d_j} \theta_{j,l} \hat{\eta}_{j,l}^{-i}(x_{i,j,l})$, and $w_{j,l}^{**}$ are adaptive weights. The additional sparsity from this approach motivates our designation of this method as sparse biniLasso.

4. Software

All analyses were performed using R (R Core Team, 2023) and RStudio (RStudio Team, 2023) for statistical computing and data visualization. The code to reproduce all the results for the simulation studies and the case study is available on the manuscript repository on our GitHub page at <https://github.com/ab-sa>. Additionally, to obtain the results for the

work by Bussy et al. (2022), we used the code provided on their GitHub page.

All simulations and analyses were conducted on a Windows-based PC with a 12th Gen. Intel(R) Core(TM) i9-12900KF processor (3.2 GHz) and a 64 GB of RAM, running Windows 11 Pro (64-bit).

5. Simulation Study

5.1 Simulation Designs

We designed a comprehensive simulation study to include additional scenarios that test the robustness and generalizability of our approach under broad and challenging conditions. Specifically, we proposed four simulation scenarios to evaluate the performance of our method. Scenarios 1 and 2 replicated the simulation design used in Bussy et al. (2022) to benchmark our findings against them, while Scenarios 3 and 4 introduced more realistic and complex conditions to assess the methods under more nuanced data-generating processes.

In Scenario 1, continuous predictors were generated from a bivariate normal distribution with zero mean and covariance matrix of Σ with an autoregressive structure, where $\Sigma_{i,j} = (0.5)^{|i-j|}$. Figure 1 A shows the original continuous distribution of predictor X_1 across observation indices ($n = 1000$). True cut-points for each predictor were determined by randomly (without replacement) selecting two deciles uniformly, resulting in categorical predictors with three levels. These predictors were then discretized into categorical variables based on the selected cut-points to be used for generating time-to-event observations. The true value of the coefficients for the categorical predictors defined as follows for $k = 1, \dots, d_j + 1$ and $j = 1, \dots, p$:

$$\beta_{j,k} = (-1)^k |c_{j,k}| - (d_j + 1)^{-1} \sum_{l=1}^{d_j+1} c_{j,l}, \quad (16)$$

where $c_{j,k} \sim N(1, 0.5)$. Figure 1 B shows the categorized version of X_1 with two cut-points (three levels), where each level has been scaled by its true coefficient from equation (16). Time-to-event data were simulated using a Weibull distribution, with the hazard function dependent on the categorized predictors only. This scenario aimed to evaluate the performance of the methods in identifying optimal cut-points for a relatively simple task when true cut-points exist for both predictors.

Building on Scenario 1, Scenario 2 extended the simulation design to include high-dimensional data with noise variables. Specifically, we generated 2 to 100 predictors from a multivariate normal distribution with zero mean and a similar covariance matrix with autoregressive structure as in Scenario 1. A sparsity parameter of 0.2 was introduced, meaning only 80% of the predictors were truly associated with the outcome, while the remaining 20% were noise variables. For all the true covariates, we set $d_j = 2$ meaning that the true relationship between these covariates and the outcome is via their three-level categorical version created in the same fashion as the one described in Scenario 1. The true coefficient values were similarly defined as in 16 for the predictors which were truly associated with the outcome, as set to zero for all the noise variables. This setup was designed to evaluate the method's

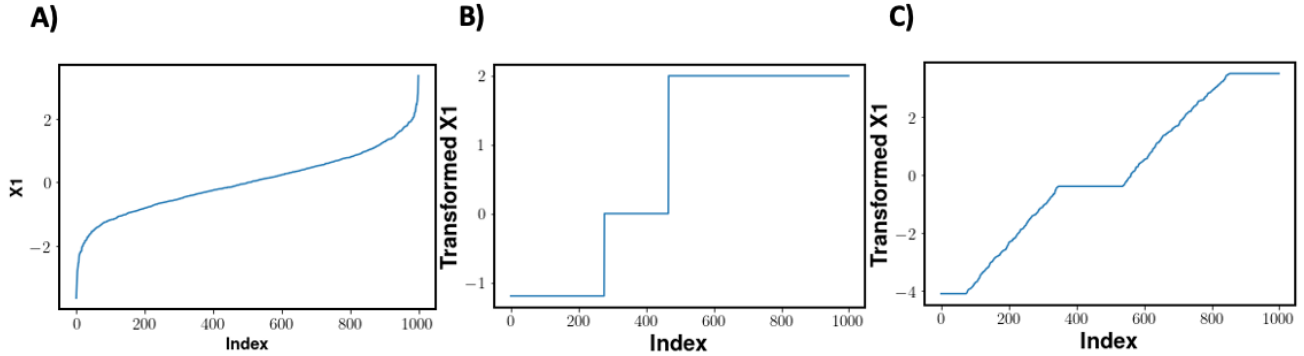


Figure 1. Illustration of simulation designs for Scenarios 1 and 3: (A) Original continuous predictor X_1 ; (B) Categorized version of X_1 with two true cut-points showing the threshold effects in Scenario 1; (C) Transformed X_1 demonstrating the gradual interval effects (‘cut-regions’) characteristic of Scenario 3.

performance in high-dimensional settings with a proportion of irrelevant predictors. Further details on the simulation mechanisms and design parameters for Scenarios 1 and 2 can be found in Bussy et al. (2022).

Scenario 3 introduced a more realistic and challenging condition by replacing true cut-points with “cut-regions”, where the effect of predictors on the outcome changed gradually within specific intervals, while remaining constant outside these regions. The data generation process for this scenario involved the following steps:

- (1) Two predictors were generated from a bivariate normal distribution, similar to Scenario 1.
- (2) The range of the predictors was expanded by multiplying them by 3 to accommodate the cut-regions.
- (3) Two deciles of each predictor were similarly randomly selected as the centres of the cut-regions.
- (4) The cut-regions were constructed by defining intervals around each center, spanning one-third of the distance between the two region centres. This divides each predictor’s range to five regions: two increasing cut-regions, and three flat regions between the cut-regions.
- (5) The mean of each predictor was derived within each three flat regions described in Step 4 in order to reflect a flat effect outside the cut-regions and a linearly increasing effect within the cut-regions.
- (6) Final predictor values were generated from a normal distribution with the means obtained in Step 5 and a fixed standard deviation (SD) of 0.2.
- (7) Time-to-event outcomes were simulated using a similar Weibull distribution as in Scenario 1 by using the transformed continuous predictors computed in Step 6.

Figure 1 C presents the transformed X_1 following the gradual-effect construction process described above. This scenario tested the methods’ ability to approximate the relationship between predictors and outcomes through categorization in the absence of true cut-points, focusing on their performance in identifying and modelling gradual changes in predictor effects.

Scenario 4 evaluates model performance under interpretability constraints by enforcing exactly two cut-points per predictor (three categories), mirroring most applications

(specially clinical) preferences for simple and limited comparison across different predictors’ levels. Using the same data generation frameworks as Scenarios 1 (true cut-points exist) and 3 (continuous effects), we assess whether models maintain reasonable performance when required to produce intuitive outputs. This constrained analysis addresses a key fact in most real applications: complex models with multiple cut-points often prove impractical, regardless of statistical performance. By comparing results across these parallel sub-scenarios, we quantify the essential trade-off between performance (e.g., predictability) and usability that arises when implementing continuous variable categorization in real-world applications.

By incorporating these scenarios, our simulation study not only replicates prior work but also extends it to more realistic and challenging conditions, providing a robust evaluation of the methods under a wide range of data-generating processes.

5.2 Comparison Framework and Benchmark Methods

Our simulation study evaluates two variants of the proposed method: (standard) *biniLasso* and sparse *biniLasso* (incorporating *uniLasso* regularization). As the primary benchmark, we include *Binacox* (Bussy et al., 2022), the only existing method suitable for high-dimensional settings with practical applicability. While alternative approaches based on multiple testing exist (e.g., Bland and Altman 1995; Lausen and Schumacher 1992), we focus specifically on scalable, regularization-based methods; readers may refer to Bussy et al. (2022) for comparisons with traditional cut-point detection approaches.

5.3 Evaluation Metrics

We evaluated the performance of our proposed method (standard and sparse) *biniLasso* against *Binacox* using the following criteria:

- **Computation Time:** We assessed the computational efficiency of *biniLasso* and *Binacox* across all simulation scenarios to compare their scalability and runtime performance.
- **Discrepancy:** In scenarios with true cut-points, we evaluate estimation accuracy using an enhanced version of the Hausdorff distance based (Harchaoui and Levy-Leduc,

2010) metric (m_1) proposed by Bussy et al. (2022). While the original m_1 metric only considered predictors with both true and estimated cut-points, our modified version incorporates all predictors by treating missing cut-points as occurring at the predictor’s minimum and maximum values. Hence no cut-points and setting cut-points at the predictor’s minimum and maximum both result in the same no relationship between the categorized predictor and the outcome. When either true or estimated cut-points are absent, we represent these cases using the predictor’s range boundaries before computing the Hausdorff distance. This approach ensures complete feature space evaluation, where predictors lacking both true and estimated cut-points naturally contribute zero distance, appropriately indicating perfect agreement when no thresholds exist. The resulting metric preserves the original interpretation while providing a more comprehensive accuracy assessment.

- **Sparsity:** In Scenario 2, which focuses on high-dimensional data with noise variables, we used the same sparsity metric as the one used by Bussy et al. (2022), m_2 , to evaluate the methods’ ability to distinguish truly associated predictors (with true cut-points) from noise variables (without true cut-points). The sparsity metric is defined as the proportion of predictors with no estimated cut-points relative to the number of predictors with no true cut-points.
- **Complexity:** We quantify model complexity using the average number of estimated cut-points per predictor, which directly reflects the interpretability of the final model in all scenarios. This metric serves as a practical measure of model parsimony, where lower values indicate simpler, more actionable decision rules.
- **Model Performance:** To evaluate the overall impact of the estimated cut-points on the fitted Cox models, we used two performance metrics: Akaike’s Information Criterion (AIC) and the Integrated Brier Score (IBS) in all scenarios. These metrics assess the trade-off between model complexity and goodness-of-fit (AIC) and the accuracy of survival predictions (IBS), respectively.

To ensure the robustness and generalizability of our findings, we conducted simulations across five different sample sizes: 300, 500, 1000, 2000, and 4000. This allowed us to evaluate the scalability and reliability of the methods under varying data sizes. Each simulation configuration was repeated 5000 times to ensure stable and reproducible results.

5.4 Simulation results

Figure 2 compares the computational efficiency and model performance of biniLasso (blue), sparse biniLasso (green), and Binacox (purple) across varying sample sizes under Scenario 1. Both biniLasso variants demonstrated substantially faster computation times than Binacox, with speed improvements ranging from 4-fold (smallest n) to 11-fold ($n = 4000$). While the IBS values suggested better predictive performance for biniLasso across all sample sizes, we observed no statistically significant differences in AIC or IBS between methods. Figure 3 displays the discrepancy metric (left) and average number of estimated cut-points for X_1 (right) across methods and sample sizes under Scenario 1. While we observed no statistically significant differences between methods, biniLasso

showed a trend toward lower discrepancy values but required more cut-points on average. The sparse biniLasso variant achieved comparable discrepancy values while maintaining greater parsimony (fewer cut-points). Binacox produced the most parsimonious models (fewest cut-points) but consistently showed the highest discrepancy values across all sample sizes. The results for the average number of estimated cut-points for X_2 were similar.

Figure 4 compares computational efficiency (left) and variable selection performance (right) across methods for $n = 1000$ under Scenario 2. Consistent with Scenario 1, both biniLasso variants demonstrated substantially faster computation times than Binacox across most dimensionalities, with the performance gap widening as P increased. The exception occurred at $P = 20$, where all methods showed comparable speeds. In variable selection, biniLasso achieved significantly better sparsity metric scores, indicating superior noise variable discrimination. The sparse biniLasso and Binacox performed similarly on this metric, though both were outperformed by standard biniLasso.

Figure 5 compares computational efficiency (left) and model fit (right) under Scenario 3, where no true cut-points exist. We evaluated models using: (1) biniLasso-estimated categories, (2) sparse biniLasso categories, (3) Binacox categories, and (4) the ground truth continuous predictors. Both biniLasso versions maintained their computational advantage over Binacox. Despite the absence of true thresholds, all categorization methods achieved AIC values comparable to the true continuous model, demonstrating their ability to capture the underlying predictor-outcome relationships through appropriate discretization. Figure 6 presents predictive performance (IBS, left) and model complexity (number of cut-points, right) under Scenario 3. All methods demonstrated comparable predictive accuracy, with no significant differences in IBS values. Similarly, we observed no meaningful variation in the average number of estimated cut-points across methods, suggesting equivalent model complexity despite their different estimation approaches.

Results for Scenario 4 mirrored those of Scenario 1, with both biniLasso variants maintaining faster computation times than Binacox while achieving comparable model performance (AIC/IBS). By design, all methods produced equally complex models (exactly 2 cut-points per predictor). However, Binacox’s single tuning parameter could not guarantee this constraint. We therefore restricted comparisons to the 10% of simulation runs where Binacox fortuitously returned two cut-points. In contrast, biniLasso’s additional tuning parameters (feature-specific weights and global regularization) enabled precise control over cut-point numbers. Complete results appear in the Appendix.

6. Case study

6.1 Datasets

To evaluate the practical performance of our method, we applied both biniLasso and Binacox to three biomedical datasets from The Cancer Genome Atlas (TCGA) platform which were previously used by Bussy et al. (2022). These datasets include breast invasive carcinoma (BRCA), glioblastoma multiforme

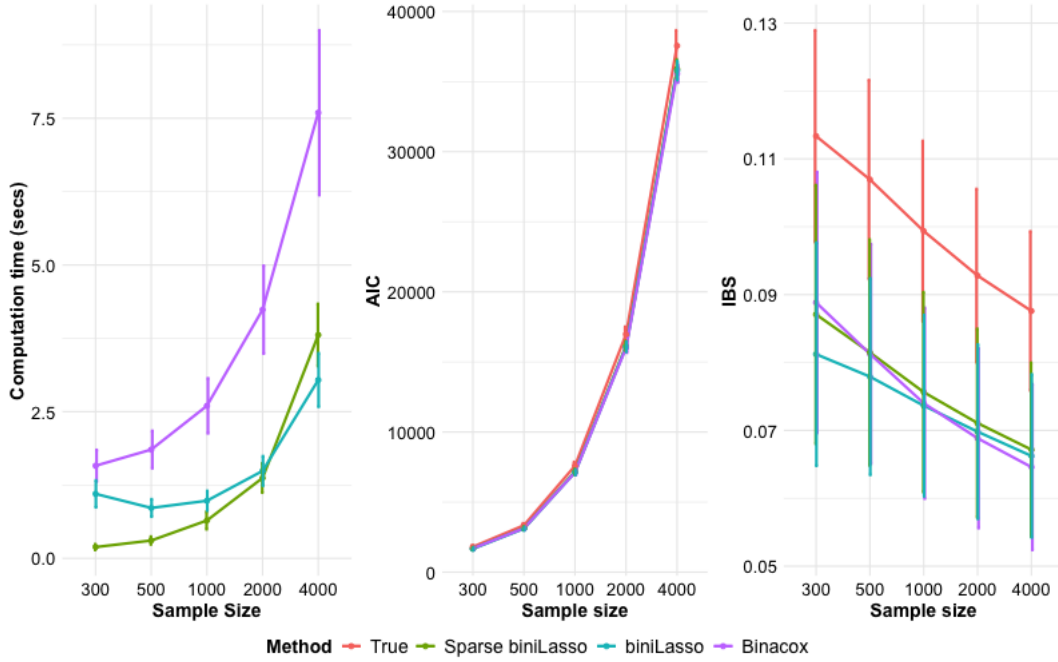


Figure 2. Comparison of biniLasso (blue), sparse biniLasso (green), and Binacox (purple) in the simulation Scenario 1: Average computing times in seconds (left), average AIC (middle), and average IBS (right) across different sample sizes (n), with vertical lines representing \pm the standard deviation (SD) based on 5000 simulated datasets. As reference, the “true” model, which used the original continuous predictors, is added (in red) to the plots.

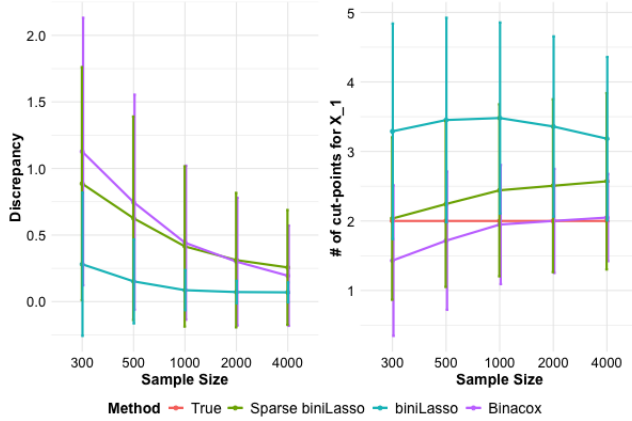


Figure 3. Comparison of biniLasso (blue), sparse biniLasso (green), and Binacox (purple) in the simulation Scenario 1: Average discrepancy (left) and average number of cut-points for X_1 (right) across different sample sizes (n), with vertical lines representing \pm the standard deviation (SD) based on 5000 simulated datasets. As reference, the “true” model, which used the original continuous predictors, is added (in red) to the plots.

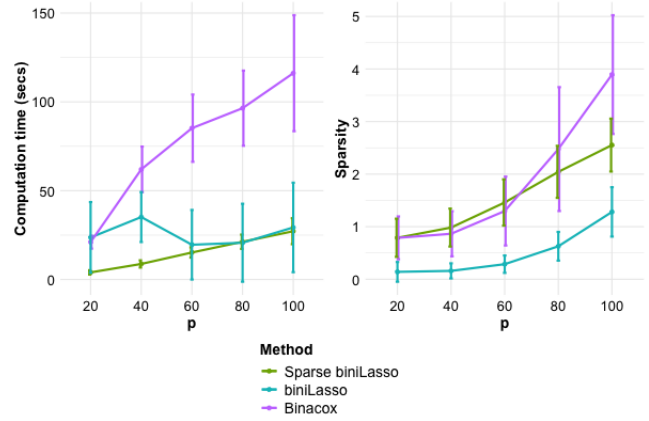


Figure 4. Performance of biniLasso (blue), sparse biniLasso (green), and Binacox (purple) in the simulation Scenario 2: Average computing times in seconds (left) and average sparsity metric (right) for varying numbers of features (P). Vertical lines represent \pm the standard deviation (SD) based on 5000 simulated datasets.

(GBM), and kidney renal clear cell carcinoma (KIRC). TCGA is a publicly available resource that leverages genomic technologies, such as large-scale genome sequencing, to advance the understanding of cancer’s molecular basis. Since their use in Bussy et al. (2022), these datasets have been updated significantly. The most recent versions include 1,231 patients

for BRCA, 391 patients for GBM, and 614 patients for KIRC, each with both gene expression and survival data. The gene expression data consist of Fragments Per Kilobase per Million mapped fragments (FPKM) unstrand values for 60,660 genes.

Following the approach of Bussy et al. (2022), we performed an initial screening step by fitting a Cox model for each gene individually and calculating the Akaike Information Criterion (AIC) and Integrated Brier Score (IBS) for each model. Genes were then ranked based on these metrics, and the top 50

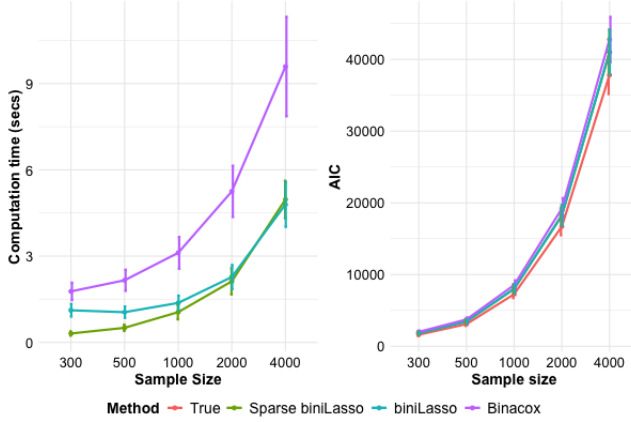


Figure 5. Performance of biniLasso (blue), sparse biniLasso (green), and Binacox (purple) in the simulation Scenario 3: Average computing times in seconds (left) and average Akaike's Information Criterion (AIC, right) across different sample sizes (n). As reference, the “true” model, which used the original continuous predictors, is added (in red) to the plots. Vertical lines represent \pm the standard deviation (SD) based on 5000 simulated datasets.

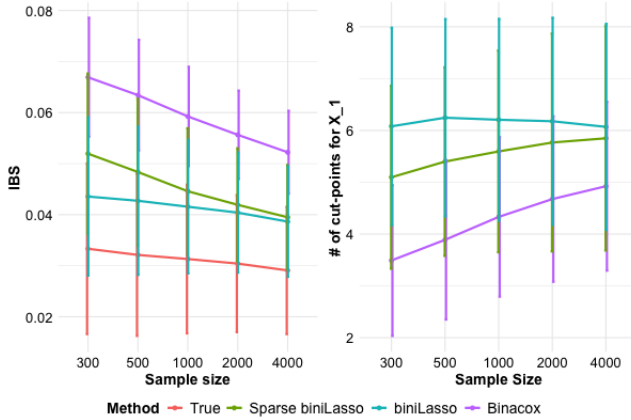


Figure 6. Performance of biniLasso (blue), sparse biniLasso (green), and Binacox (purple) in the simulation Scenario 3: Average IBS (left) and average number of estimated cut-points for X_1 (right) across different sample sizes (n). As reference, the “true” model, which used the original continuous predictors, is added (in red) to the IBS plot. Vertical lines represent \pm the standard deviation (SD) based on 5000 simulated datasets.

genes from each ranking were selected, resulting in up to 100 unique genes per dataset (due to overlap between the top 50 genes from each metric). Finally, the selected genes were standardized before applying biniLasso and Binacox. A summary of the datasets after the screening step is provided in Table 1.

6.2 Estimated cut-points

We applied both biniLasso and Binacox to each dataset after the screening step. For both methods, in a similar fashion as our simulation study, we set number of bins to 50 for

Table 1

Summary of the breast invasive carcinoma (BRCA), glioblastoma multiforme (GBM), and kidney renal clear cell carcinoma (KIRC) datasets obtained from The Cancer Genome Atlas (TCGA).

Data	n	No. of genes	No. of selected genes
BRCA	1231	60660	96
GBM	391	60660	91
KIRC	614	60660	92

all predictors (i.e., $d_j = 50$ for all j). Table ?? reports the estimated cut-points for the GBM dataset. biniLasso detected a single cut-point for 13 genes and two cut-points for 3 genes in this dataset. The estimated cut-points for the BRCA (1 gene) and KIRC (13 genes) datasets are detailed in Tables S1 and S2 in the Supplementary Materials. In contrast, Binacox failed to detect any cut-points for the GBM and BRCA datasets (and therefore, no useful predictions for these two datasets either) and identified a single cut-point for 16 genes in the KIRC dataset, none of which overlapped with those detected by biniLasso.

Table 2

Estimated optimal cut-points for the KIRC dataset identified by biniLasso, sparse biniLasso, and Binacox.

Genes	biniLasso	Sparse biniLasso	Binacox
DLGAP1	.	.	-0.165
MGAM	.	.	-0.266
CUBN	0.660	0.660	-0.201
TXLNA	0.087, 0.191	0.191	.
IMPDH1	1.615	1.615	.
LIN54	-0.321, 0.044	.	.
NCKAP5L	.	.	-0.032
NUMBL	.	1.078	.
CYP3A7	-0.557	.	.
MBOAT7	-0.112, 0.879	0.879	.
ADM5	1.249	.	.
USB1	0.126	.	.
SNORD100	-0.126	.	.
EIF4EBP2	0.408	0.339	0.409
SORBS2	-0.654	.	-0.653
GIPC2	.	.	-0.110
SELENOP	.	.	-0.420
ANAPC7	0.428, 0.603	0.428	.
SLC16A12	-0.943	.	-0.735
DONSON	0.071	.	0.071
MSH3	-0.384	.	-0.386
SGCB	0.199	0.199	-0.330, 0.200
CDCA3	.	0.589	.
ADH5	.	.	-0.271
SLC2A9	-0.067	-0.067	-0.137
CKAP4	1.305	1.305	.
HJURP	0.178	0.187, 0.491	.
IL4	1.111	1.111	.
MXD3	.	.	0.001
SLC27A2	.	.	-0.179
CARS1	0.255	0.255	0.258

6.3 Model performance

To evaluate the impact of the detected cut-points on the overall performance of the Cox model, we categorized genes

with at least one detected cut-point for each method and fitted Cox models using these categorized predictors. Table 3 summarizes the performance metrics, including AIC, IBS, and the Concordance Index (C-index) along with its estimated SD, for the fitted Cox models based on the categorized gene expression predictors for both biniLasso, sparse biniLasso, and Binacox. biniLasso consistently outperformed Binacox across all three datasets, achieving the lowest AIC and IBS values and the highest C-index values.

7. Discussion

In this work, we present biniLasso and its sparse variant (sparse biniLasso) as novel extensions of the Binacox approach, designed for efficient multi-cut-point detection in high-dimensional Cox models. Our comprehensive simulations demonstrate that both biniLasso versions outperform Binacox computationally, achieving 4-11 \times faster processing times while maintaining or improving accuracy in cut-point identification and model performance. The standard biniLasso proves particularly effective for detecting multiple cut-points per feature, capturing complex predictor-response relationships, while sparse biniLasso offers enhanced interpretability through its uniLasso-regularized feature selection. We validate these advantages through application to three high-dimensional genomic datasets, confirming their practical utility in real-world biomedical research.

The cumulative binarization approach used in biniLasso addresses several limitations of conventional binarization methods for categorizing continuous covariates. Traditional binarization methods, which rely on fixed intervals or percentiles, are often sensitive to the choice of interval boundaries and can lead to small sample sizes in certain bins, reducing statistical power and introducing bias (Royston et al., 2006). In contrast, the nested intervals in biniLasso are less sensitive to boundary choices, allowing for more flexible and precise cut-point estimation without compromising sample size. This approach mitigates issues such as residual confounding and loss of precision, particularly in the outer intervals of the data range (Naggara et al., 2011).

Our results suggest distinct application domains for each method variant. The sparse biniLasso is particularly advantageous in exploratory analyses where the optimal number of cut-points is unknown, as its uniLasso regularization automatically determines appropriate model complexity while maintaining clinical interpretability. Conversely, standard biniLasso proves more suitable when prespecified cut-point requirements exist such as clinical decision tools requiring exactly three risk categories (low/medium/high), due to its precise control over threshold quantities. This methodological division accommodates both data-driven discovery and implementation-ready model development within the same analytical framework.

Our study has some limitations. First, the performance of biniLasso relies on the pre-specified set of cut-point candidates, which may not always capture the true underlying structure of the data. Second, while biniLasso is computationally efficient, its scalability to ultra-high-dimensional datasets (e.g., millions of features) remains to be tested. Finally, the method assumes that the relationship between predictors

and outcomes can be adequately modelled using cut-points, which may not hold for all types of data. Future work could explore adaptive methods for selecting cut-point candidates and extend biniLasso to handle more complex data structures.

How can this approach be utilized in real-world applications? We strongly advocate for first identifying the optimal relationship between predictors and the risk of outcomes, irrespective of its immediate clinical interpretability. This can be achieved using an additive Cox proportional hazards model, such as the Cox-based Generalized Additive Model (CGAM), which leverages smoothing spline-based machine learning algorithms (Hastie and Tibshirani, 1990; Wood et al., 2016; Bender et al., 2018). In this approach, continuous predictors are included in the Cox model, and smoothing splines are applied to flexibly estimate potentially non-linear, data-driven relationships between predictors and outcomes. Generalized cross-validation can be used during model fitting to determine the appropriate level of smoothness, thereby avoiding overfitting while maintaining flexibility.

For generating clinically actionable insights, we recommend to categorize continuous predictors based on identified cut-points by biniLasso and then fitting a standard Cox proportional hazards model using the categorized predictors instead. This approach balances interpretability and performance, making it more suitable for practical applications. To evaluate the trade-off between interpretability and predictive accuracy, model performance metrics such as AIC or IBS can be used to compare the simplified Cox model with the more flexible CGAM. This ensures that the results remain both scientifically robust and clinically relevant.

In conclusion, biniLasso represents a significant advancement in the analysis of high-dimensional survival data, offering a computationally efficient and interpretable approach for identifying multiple cut-points per feature. Its ability to handle complex relationships while maintaining high predictive accuracy makes it a valuable tool for both research and clinical applications. By combining the flexibility of non-parametric methods with the simplicity of categorized predictors, biniLasso bridges the gap between statistical rigour and practical usability, paving the way for more effective prognostic modelling in high-dimensional settings. Future research should focus on extending its applicability to ultra-high-dimensional data and exploring adaptive methods for cut-point selection to further enhance its utility.

ACKNOWLEDGEMENTS

REFERENCES

- Alaya, M., Bussy, S., Gaiffas, S., and Guilloux, A. (2019). Binarisity: a penalization for one-hot encoded features in linear supervised learning. *Journal of Machine Learning Research* **20**, 1–118.
- Bender, A., Groll, A., and Scheipl, F. (2018). A generalized additive model approach to time-to-event analysis. *Statistical Modelling* **18**, 299–321.
- Bland, M. and Altman, D. (1995). Multiple significance tests: the bonferroni method. *BMJ* **310**, 170.
- Bussy, S., Alaya, M., Jannot, A.-S., and Guilloux, A.

Table 3

Performance metrics for Cox models fitted using categorized gene expression predictors derived from the estimated cut-points of biniLasso, sparse biniLasso, and Binacox for the BRCA, GBM, and KIRC datasets.

Dataset	Metric	biniLasso	Sparse biniLasso	Binacox
BRCA	AIC ¹	1953	1979	2109
BRCA	IBS ²	0.082	0.096	0.163
BRCA	C-index ³ (SD)	0.548 (0.015)	0.5 (0)	
BRCA	No. of cut-points	55	36	0
GBM	AIC	2737	2812	3026
GBM	IBS	0.030	0.037	0.064
GBM	C-index (SD)	0.726 (0.016)	0.5 (0)	
GBM	No. of cut-points	60	48	0
KIRC	AIC	2081	2078	2108
KIRC	IBS	0.146	0.158	0.154
KIRC	C-index (SD)	0.769 (0.016)	0.698 (0.018)	
KIRC	No. of cut-points	30	21	18

¹ Akaike’s Information Criterion

² Integrated Brier Score

³ Concordance Index

(2022). Binacox: automatic cut-point detection in high-dimensional cox model with applications in genetics. *Biometrics* **78**, 1414–1426.

Chatterjee, S., Hastie, T., and Tibshirani, R. (2025). Univariate-guided sparse regression.

Cheang, M., Chia, S., Voduc, D., Gao, D., and et al. (2009). Ki67 index, her2 status, and prognosis of patients with luminal b breast cancer. *Journal of National Cancer Institute* **101**, 736–750.

Cox, D. (1972). Regression models and life-tables. *Journal of the Royal Statistical Society* **34**, 187–202.

Gaïffas, S. and Guilloux, A. (2012). High-dimensional additive hazards models and the Lasso. *Electronic Journal of Statistics* **6**, 522 – 546.

Harchaoui, Z. and Levy-Leduc, C. (2010). Multiple change-point estimation with a total variation penalty. *American Statistical Association* **105**, 1480–1493.

Hastie, T. and Tibshirani, R. (1990). *Generalized Additive Models*. Chapman & Hall/CRC.

Lausen, B. and Schumacher, M. (1992). Maximally selected rank statistics. *Biometrics* **48**, 73–85.

Naggara, O., Raymond, J., Guilbert, F., Roy, D., Weill, A., and Altman, D. (2011). Analysis by categorizing or dichotomizing continuous variables is inadvisable: An example from the natural history of unruptured aneurysms. *American Journal of Neuroradiol* **32**, 437–440.

O’Brien, S. M. (2004). Cutpoint selection for categorizing a continuous predictor. *Biometrics* **60**, 504–509.

Philip, W., Anderson, D., Rodger, M., Ginsberg, J., and et al. (2000). Derivation of a simple clinical model to categorize patients probability of pulmonary embolism: Increasing the models utility with the simplified d-dimer. *Thrombosis and Haemostasis* **83**, 416–420.

Royston, P., Altman, D., and Sauerbrei, W. (2006). Dichotomizing continuous predictors in multiple regression: a bad idea. *Statistics in Medicine* **25**, 127–141.

Safari, A., Helisaz, H., Salmasi, S., Adalakun, A., De Vera, M., and et al. (2024). Association between oral anticoagu-

lant adherence and serious clinical outcomes in patients with atrial fibrillation: A long-term retrospective cohort study. *Journal of the American Heart Association* **13**, e035639.

Salmasi, S., Safari, A., De Vera, M., Hogg, T., and et al. (2024). Adherence to direct or vitamin k antagonist oral anticoagulants in patients with atrial fibrillation: a long-term observational study. *Journal of Thrombosis and Thrombolysis* **57**, 437–444.

Wood, S., Pya, N., and Saffken, B. (2016). Smoothing parameter and model selection for general smooth models. *Journal of the American Statistical Association* **111**, 1548–1563.

Wu, J. and Coggeshal, S. (2012). *Foundations of Predictive Analytics*. Chapman and Hall/CRC.

SUPPORTING INFORMATION

Tables S1 and S2 summarize the number of genes with detected cut-points, including single and multiple cut-points, as well as their specific values for the gene datasets BRCA and KIRC, respectively.

Table S1

Estimated optimal cut-points for the BRCA dataset identified by biniLasso and Binacox.

Genes	biniLasso	Binacox
ABCB5	-0.42	.

Received October 2004. Revised February 2005.

Accepted March 2005.

Table S2

*Estimated optimal cut-points for the KIRC dataset identified
by biniLasso and Binacox.*

Genes	biniLasso	Binacox
CUBN	-1.01	.
TXLNA	-1.58	.
NUMBL	-0.88	.
CYP3A7	-0.52	.
EIF4EBP2	-1.63	.
SORBS2	-1.71	.
ANAPC7	-1.19	.
SLC16A12	-1.11	.
CDCA3	-0.59	.
SLC2A9	-0.95	.
HJURP	-0.60	.
IL4	-0.77	.
CARS1	-1.45	.
RUNDC3B	.	-1.05
GGACT	.	-0.48
SEMA3D	.	-0.62
KMT5A	.	-1.43
Z83745.1	.	-0.87
PTPRB	.	-1.32
GIPC2	.	-1.37
FBXL5	.	-1.45
EHHADH	.	-1.23
AMOT	.	-1.45
MSH3	.	-1.31
OSBPL1A	.	-1.65
PLPP3	.	-1.44
SLC52A2	.	-1.11
RORA	.	-1.22
METTL24	.	-1.13